Proceedings of the ASME 2012 International Design Engineering Technical Conferences & Computers and Information in Engineering Conference
IDETC/CIE 2012
August 12-15, 2012, Chicago, IL, USA

DETC2012-71436

COOPERATIVE MICROMANIPULATORS FOR 3D MICROMANIPULATION AND ASSEMBLY

David J. Cappelleri*
Multi-Scale Robotics & Automation Laboratory
Department of Mechanical Engineering
Stevens Institute of Technology
Hoboken, NJ 07030
Email: David.Cappelleri@stevens.edu

Zhenbo Fu
Multi-Scale Robotics & Automation Laboratory
Department of Mechanical Engineering
Stevens Institute of Technology
Hoboken, NJ 07030
Email: zfu@stevens.edu

ABSTRACT

In this paper we demonstrate coordinated control of multiple micromanipulators for use in automated 3D micromanipulation and assembly tasks. We build on our previous work on caging micromanipulation by using a similar methodology and extend it to the 3D case. Simultaneous movements of the coordinated micromanipulators normal to the caging polygon allows for the transition of 2D planar micro-caging grasps to micro-force closure grasps suitable for 3D micro-transporting tasks. Experimental results illustrate the success and accuracies of both the micro-grasps' transitions and 3D pick-and-place tasks. Finally, the new 3D transportation primitive is used in conjunction with our previous 2D micromanipulation primitives and an encoded XY stage to semi-autonomously execute some representative 3D microassembly tasks.

INTRODUCTION

Research on automated gripping and manipulation techniques for microassembly applications is becoming more and more important in recent years coinciding with the manufacturing trends to create smaller and cheaper products with increased throughput [1]. There is a much related work pertaining to pick-and-place microassembly tasks using micro-gripping techniques and strategies [2–8]. Manipulators at the micro-scale are limited in their degrees-of-freedom when compared to their macro-scale counterparts [9]. Furthermore, the presence of Van der Walls forces at the micro-scale can induce sticking effects between the end-effectors and micro-parts, thus, making the release and precise placements of parts difficult [10, 11]. Some researchers have pursed 3D microassembly cells with with the use of micro-snap fasteners on micro-grippers, parts, and/or mounting substrates to eliminate this problem [12–21]. Others have investigated pop-up or foldable 3D MEMS parts and assemblies. In [22], the parts are manufactured in a planar-fashion as multiple plates constrained by hinges so that the assembly process consists of a single degree of freedom motion actuated with hydrodynamic forces. In [23], a stretchable circuitry is created on an origami module with compliant joints for controlled folding. Another interesting alternative approach is hybrid microassembly combining tweezer-type microgrippers and droplet self-alignment with capillary forces [24].

However, it may not be desired or even feasible to always to be able to design parts with the requisite features for micro-snap fastening, with the necessary joints, or that are hydrophilic, that the methods mentioned above require. Therefore, rather than utilizing micro-grippers or relying on specialized part features or assembly substrates to realize 3D micromanipulation and microassembly tasks, we are interested in utilizing coordinated movements of multiple micromanipulators with simple point probe-type end-effectors. A microassembly cell like this is flexible enough to handle both 2D and 3D micromanipulation and assembly tasks. While a multi-fingered micromechanism for

*Address all correspondence to this author.

Copyright © 2012 by ASME

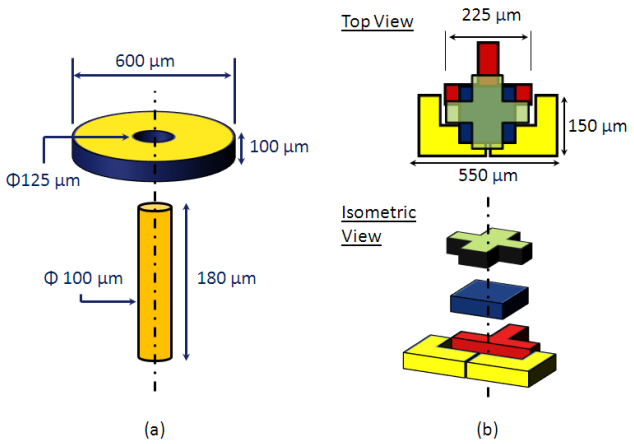

FIGURE 1. Representative 3D microassembly problems to be solved. (a) 3D (vertical) peg-in-the-hole problem of placing a micro-ring part on a micro-post; (b) 3D micromanipulation problem, that includes a planar peg-in-hole subproblem, in order to to create ground plane of micro-parts for stacking of additional mirco-parts

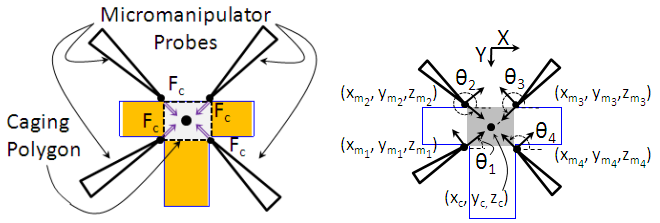

(a) FD micro-caging grasp. (b) Local micromanipulator coordinates on a caging polygon.

FIGURE 2. Feature-defined (FD) micro-caging grasp schematic and micromanipulator reference frames for transport primitives.

coordinated micro/nano manipulation has been presented in [25], it has a very limited range of motion and is not well-suited for high throughput assembly of micro-scale components and devices. The microassembly cells presented in [26–28] utilize multiple manipulators as well but they are generally each used for individual operations and not cooperating to manipulate the same part at the same time and/or with specialized micro-snap fasteners, parts, and substrates. A vision-based 3D micromanipulation and microassembly task has been demonstrated in [29, 30] with two coordinated manipulators with point probes while in [31], two manipulators with point probes have been teleoperated in order to carry out a 3D microassembly task.

Cooperative manipulation is common at the macro-scale using concepts of form and force closure in order to manipulate objects [32–34]. It is also possible to use conditional force closure to transport an object by pushing it from an initial position to a goal position [35, 36]. Conditional force closure makes use of both the manipulation forces generated by contacts from the robots as well as the external forces acting on the object, such as friction and gravity. Object closure or caging is variation of this. It only requires that the objected be caged by the robots and confined to a compact set in the configuration space [37, 38]. Multirobot manipulation of non-circular objects and cooperative manipulation in environments with obstacles has been demonstrated in [38, 39] with macro-scale mobile robots. We have recently used similar principles and applied them to 2D micromanipulation and assembly tasks, creating a new micro-scale caging transport primitive with up to four cooperative micromanipulators with point-probes [40]. It can be coupled with our prior work [41–43] and [44] to construct rotational and 1D translation motion primitives to use with this caging transport primitive to carry out a sample microassembly tasks [45]. In this paper, we build on our previous methodology and extend it to the 3D case for use in automating the 3D micromanipulation and microassembly tasks shown in Fig. 1. We examine the reliability of transitioning from a micro-caging grasp to a force closure grasp, the stability of the grasps during 3D transport, and explore coordinated movements with our encoded XY stage in order to experimentally achieve the 3D microassemblies of interest.

PROBLEM FORMULATION

The general problem formulation from our previous work in [40] remains the same here except we must adapt it for the 3D manipulation case. We consider a group of N micromanipulators ($N \leq 4$) with single point probes (robots) operating in an XYZ 3D workspace with kinematics given by: $\dot{q}_{m_i} = u_{m_i}$, where $q_{m_i} = (x_{m_i}, y_{m_i}, z_{m_i})^T$ and u_{m_i} denote the i^{th} tip position of the manipulator's probe and corresponding control input. We assume each manipulator is localized in a global coordinate frame. Our objective is to design a set of control inputs to enable a team of N micromanipulators to surround, grasp, and transport an object to a desired location and orientation in both 2D and 3D space while avoiding obstacles (other micro-parts) in the environment in order to solve the representative microassembly problems depicted in Fig.1.

2D MICRO-CAGING TRANSPORT

When using caging micromanipulation for planar transporting a micro-part of interest, we assume that if the cage is maintained, the part's centroid, (x_p, y_p, z_p), will always lie within a caging polygon (Fig. 2(a)). Guarantees of part rotation are not made but they are bounded utilizing caging parameters driven by the part geometries and functions of the micro-caging ε-ring distance [45]. The microrobotics test-bed used here (Fig. 4(a)) allows for use of up to $N = 4$ manipulators for micro-scale caging transport operations, as seen in Fig. 2(b).

To translate the 2D center position of the cage, (x_c, y_c), we

Copyright © 2012 by ASME

must map the control inputs, $U_{cage} = [u_{x_c} u_{y_c} 0]^T$, to the local frames of the micromanipulators being utilized. Each manipulator control input, u_{m_i}, must be prescribed in the local coordinate frame orthogonal to the manipulator's orientation (θ_i, i = 1,..,4, as defined in Fig. 2(b)) and are given by: $u_{m_i} = T_i U_{cage} = [u_{x_{m_i}} u_{y_{m_i}} u_{z_{m_i}}]^T$, where T_i corresponds to the transformation matrix for each manipulator: $T_1 = R_x(180^\circ)R_z(\theta_1)$, $T_2 = R_x(180^\circ)R_z(\theta_2)$, $T_3 = R_z(\theta_3)$, and $T_4 = R_z(\theta_4)$. In these expressions, $R_x(\beta)$ and $R_z(\beta)$ represent 3D-rotation matrices about the x and z axes, respectively, by the prescribed angle β [46].

3D COOPERATIVE TRANSPORT

The micro-caging grasps developed in our previous work [40, 45] are not designed to provide force closure on the micro-parts of interest since they are to be utilized for planar transport tasks. However, for 3D transport tasks, force closure is needed. In order to plan the grasp points for the micro-force closure grasps needed for the 3D manipulation case, we will start first from a micro-caging grasp (Fig. 3(a)) and then transition to a micro-force closure grasp. We can follow the algorithm presented in [45] that uses the features of the part of interest in order to determine the number and placement of the micromanipulators needed to form an appropriate micro-caging grasp. This algorithm essentially looks to place the probe tips at convex corners of the parts, if they exist, or surrounding the non-convex corners of the part, in order to provide opposing forces on either side of the object similar to a parallel jaw gripper. The probe tips surround a caging polygon region of the part and are located an ε distance from edges of the part. An example of this situation is shown in Fig. 3(a) in both top and isometric views. To transition from the micro-caging grasp to the micro-force closure grasp, we actuate each micromanipulator to move a $\sqrt{2} \cdot \varepsilon + \delta$ distance along their local x-axis direction (i.e., the direction of the manipulator center-lines shown in Fig.3(a)). The value for δ needs to be sufficient to provide a stable grasp, but not too large to squeeze the part too much. The micromanipulators also need to close the desired amount simultaneously in order to provide uniform forces on all directions of the part for stable transport and release. Note: probes with point contacts are used here to minimize the contact surface area between the end-effector and part of interest in order to mitigate against part stiction. If the coordination of the grasps opening/closing is off, it can result in the contact points of the probes to move from the tips to points on the shank of the probe with a larger contact area which can lead to an increase in part stiction. Fig.3(b) shows top and isometric views of the manipulators after transitioning into a micro-force closure grasp on a micro-part. Once the micro-force closure grasp has been established, the simultaneous movement of the micromanipulators along the Z-axis will move the part out of the XY plane (Fig.3(c)). From there, the micromanipulators can be commanded to cooperate in a similar manner as in the case of 2D micro-caging transport to move the part above its desired location. Once hovering above a desired location, the process can be reversed in order to precisely place the part either on the substrate or into an assembly position. Again, too tight of a micro-force closure grasp or misaligned probe tips can result in part stiction and/or inaccurate final part placements.

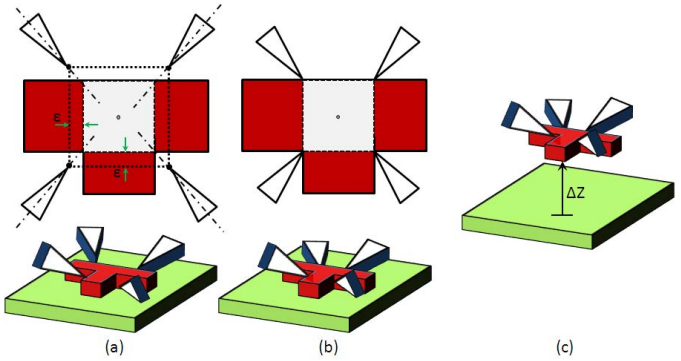

FIGURE 3. Transitioning from a 2D micro-caging grasp to a micro-force closure grasp for 3D transport tasks. (a) Initial manipulator placement in a micro-caging grasp configuration; (b) After successful transition to micro-force closure grasp by actuating each micromanipulator along its local x-axis direction; (c) Coordinated movements of the micromanipulators along the global Z-axis results in lifting the part out of the XY plane.

EXPERIMENTAL SETUP

The microrobotics test-bed used here is shown in Fig. 4(a). It consists of an inverted optical microscope (Nikon Ti-U), automated XY stage with encoders (Nikon Ti-S-ER), two CCD cameras (Point Grey Research Flea2, Flea3), and four computer-controlled manipulators (Sutter Instruments MPC-285), and customized controllers. The XY stage has a travel range of 110 mm $\times$ 75 mm, in the X and Y directions, respectively. It can move in both course position and fine positioning modes, with a minimum resolution of 100 nm. The manipulators have 3 controllable degrees-of-freedom with a minimum step size of 62.5 nm with a travel range of 1" on each axis. A custom LabView-based control program was development to allow for real-time vision position tracking, manual, and automated, simultaneous control of all the manipulators in the system. The graphical user interface (GUI) for the control program is shown in Fig. 4(b). The manipulators are outfitted single tip tungsten probe end-effectors with 5 μm diameter tips. Manipulation and assembly tests were performed on parts made from SU-8 photoresist (*www.microchem*) with the planar dimensions shown in Fig. 5. The part thicknesses are about 50 μm. A 4X objective was used in the microscope along with a 1.5X zoom providing a field of view of approximately 2230 μm X 1650 μm. The camera images provide a resolution of about 1.6 μm/pixel. Using this test-bed, experimental

Copyright © 2012 by ASME

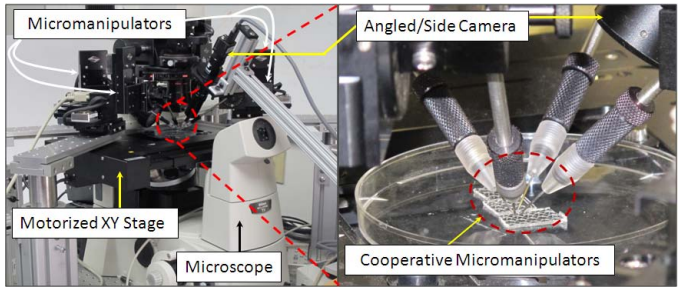

(a) Microrobotics test-bed hardware

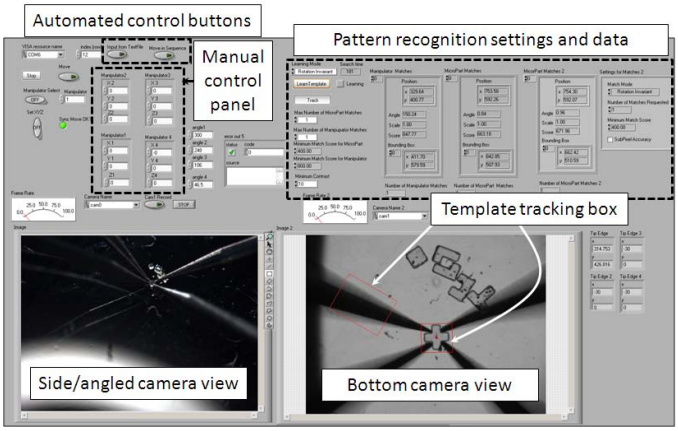

(b) Microrobotics test-bed control GUI

FIGURE 4. Flexible microbobotics test-bed.

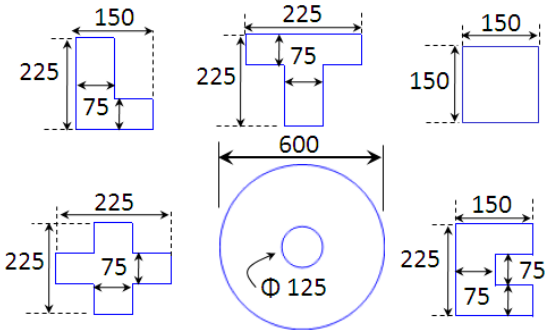

FIGURE 5. Micro-parts and dimensions used for testing. Note: all dimensions are in microns

3D manipulation tests for each part were conducted as well as the representative assembly tasks executed.

3D TRANSPORT TESTS

3D transport tests were conducted on the micro-parts shown in Fig.5. A 3D transport test consists of the following subtasks. The first component of the transport test is to have the cooperative manipulators successfully transition from a micro-caging grasp to a micro-force closure grasp for a particular micro-part

TABLE 1. 3D Transport Tests Results

Part Type	C2C? (%)	Successful? (%)	Ave. Max Error Δ X (μm)	Ave. Max Error Δ Y (μm)	Ave. Max Error $\Delta\,\theta$ (°)
Square	100	100	16	9	12
L	100	100	12	11	11
T	100	100	12	10	15
Cross	100	100	17	3	10
U	100	0	NA	NA	NA
Ring	100	75	6	9	NA

Note for each trial: Δ Z movement = $\pm$ 100 μm; 3D Transport distance = 600 μm

of interest. If/once the caging-to-closure (C2C) subtask was successful, the manipulators translate the part along the Z-direction a distance of 100 μm above the substrate. Once suspended in the air, the manipulators are commanded to cooperatively translate the part a distance of 600 μm along the X-direction. Then the part is lowered 100 μm back down to the substrate and the manipulators are simultaneously retracted to release the part. The final position and orientation of the part is compared with the goal end position to calculate the errors for the 3D transport task. For a starting configuration of $(x_p, y_p, z_p, \theta_p)$, the goal position is simply $(x_p + 600, y_p, z_p, \theta_p)$. At least 5 trials for each part were conducted and the results are shown in Table1. The second column of Table 1 lists the % of the trials for the part of interest with successful C2C transitions; column 3 reports the % of the trials with successful 3D transport; the last three columns report the average maximum placement errors at the end of the test. A successful C2C transition is defined by the fact the part does not initially get pinched unevenly causing it to escape the cage and that once the grasp is established, the part is stable enough to be able to be successfully translated (lifted) in the z-direction. For the grasp transition subtask, we used an $\varepsilon = 25$ μm and a $\delta = 3$ μm. The choice of δ is based on the size of the part, type of part (rigid), and was empirically determined. Screenshots from some of the transport tests are shown in Fig.6.

The part placements (XY coordinates) after the transport tasks are all very accurate, with less than 5% errors with respect to its overall transport distance (600 μm). The orientation changes ($\Delta\theta$'s) are due to small amounts of stiction upon release of the parts and the errors are all less than 5% as well. We cannot report on any quantitative accuracies of the z-axis moves at this time other than just observing encoder feedback information from taken directly from the micromanipulators. Qualitatively though, if the part has a successful C2C transition, it is able to be moved along the z-direction.

From Fig.6 and the data in the Table 1 however, it is evident that some parts were not able to be successfully transported in the manner we had hoped. While the C2C transitions appeared successful, inaccuracies in the translation distance of any or all of the micromanipulators can cause the parts to become unstable during the transport and fail. This was particularly a problem

Copyright © 2012 by ASME

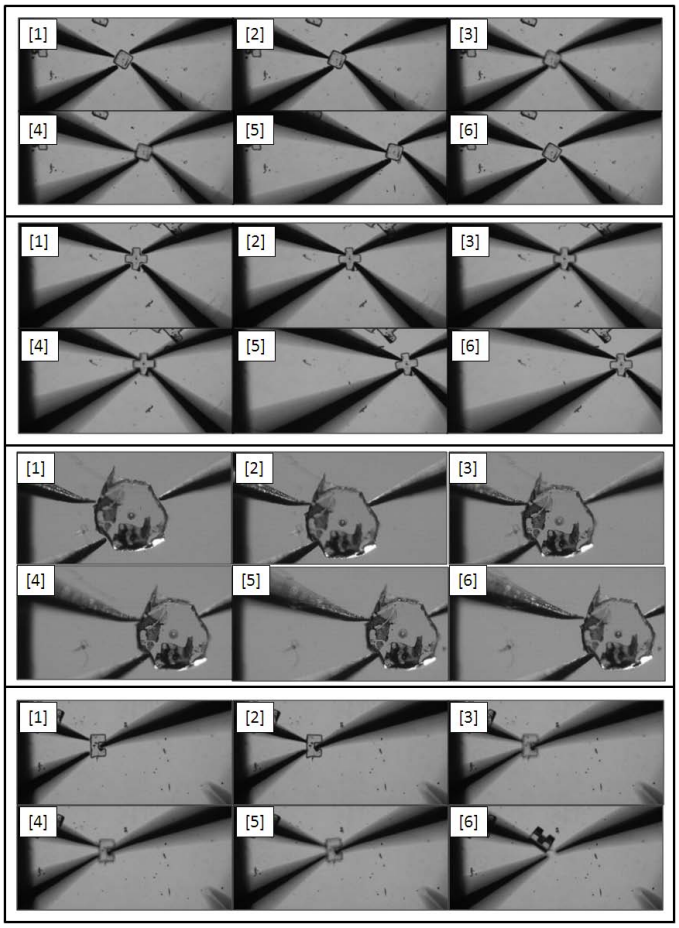

FIGURE 6. 3D transport tests. From the top panel to the bottom panel: screenshots of a trial for a square, cross, ring, and u-shaped micro-parts, respectively.

in the case of the U-part (Fig.6, bottom panel). Without force information at the contacts, it is not possible to determine if a proper force distribution is maintained at each contact throughout the transport distance.

However, in order to accomplish our desired assembly tasks we need an alternative approach to increase the stability of the 3D transport primitive. We have demonstrated successful C2C transitions at the beginning and end of the 3D transport task along with accurate part placements and out-of-the-plane movements with the cooperative manipulators. If we can couple these the movements of the encoded XY stage in the test-bed, we can achieve robust 3D transport. We can simply replace the translation of the probes with a translation of the XY stage. This will move the goal position under the suspend part rather than translating the part to above the goal position. In order to use the XY stage as part of the 3D transport primitive, we conducted a series of XY stage characterization tests. For these tests, we directed the XY stage to translate in a 600 μm $\times$ 600 μm square path and tracked the positions of a micro-part in the field of view. Table 2 shows the results for 5 trials of these tests, while Fig 7 shows some screensshots of the part trajectory from one of one such stage characterization test. The encoders of the XY stage are extremely accurate. The stage can be commanded to move in as little as 100 nm increments. Therefore, the maximum errors shown in Table 2 are negligible and the XY stage can be reliably used as part of our manipulation and assembly plans.

TABLE 2. XY Stage Characterization Tests

Trial #	Δ X (μm)	Δ Y (μm)	Max % Error X-axis	Max % Error Y-axis
1	600	600	0.10	0.10
2	600	600	0.20	0.15
3	600	600	0.21	0.16
4	600	600	0.10	0.11
5	600	600	0.09	0.04

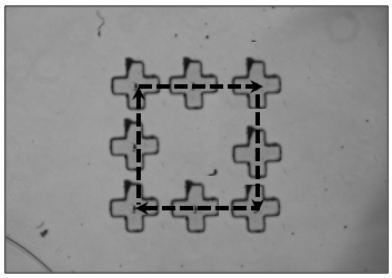

FIGURE 7. XY stage characterization: screenshots from 600 μm square path test

MICROASSEMBLY TESTS

Based on the results of the 3D transport and XY stage characterization tests, we can now plan and execute 3D micromanipulation plans to execute the microassembly tasks pictured in Fig.1. Each plan will be described now along with results of the experimental trials performed to execute these tasks. The assembly trials were executed semi-autonomously, with the operator placing the micromanipulators into position at the beginning of each primitive and then the system autonomously executing the primitives.

3D Peg-in-the-hole Assembly

The 3D peg-in-the-hole assembly task (Fig.1(a)) has a task tolerance of 25 μm. The manipulation plan for the task is the following:

Manipulation Plan

1. Start from micro-caging grasp on ring and transition to micro-force closure grasp.
2. Cooperatively move manipulators 200 μm in +Z-direction.

Copyright © 2012 by ASME

3. Translate the (3a) part or (3b) substrate to align the center of the target post to the center of the ring.
4. Lower the ring on to the post by cooperatively moving the manipulators 100 μm in the (-)Z-direction.
5. Retract the manipulator probes to release the part.

This manipulation plan (with Step 3a to translate the part) was followed experimentally and the micro-ring was able to be successfully placed in the micro-post a total of four times out of four attempts. Screen-shots from one of these experiments are shown in Fig. 8(a) and a close-up (10X) image of the final assembled micro-ring on the micro-post is shown in Fig. 8(b). The execution of the microassembly task was performed semi-autonomously, as described above. Fully automating the system will decrease the operation time for task execution and increase reliability and yield. Currently, the task execution time for the manual procedure is about 25 seconds with manipulator speeds of 425 μm/sec. Conservatively, we can expect to be able to reduce this to 15 seconds or less with a fully automated system and increased manipulator speeds.

This same assembly task has also been executed utilizing the XY stage to translate the substrate (Step 3b). In this case, instead of translating the center of the part to hover over the center of the post in step three of the manipulation plan, we translated the substrate below the part with the stage controls to align the centers of the ring and post. A nice feature of this scenario is that it allows for the assembly location to reside outside of the same field of view of the initial location of the micro-parts. Once the micro-part is grasped and raised above the substrate, the XY stage can be used to for large translations to bring the assembly location and part into the same field of view for precise positioning. Note: the speed of the XY stage was set to 460 μm/sec for these experiments.

3D Positioning & Stacking

The 3D positioning and stacking assembly problem (Fig.1(b)) has a task tolerance of 75 μm. For this task, we start with micro-parts all in their goal orientation in a horizontal line at the top of the field of view of the microscope (Fig.9(a)(a)-1). The first L-shaped piece is moved into position first using the micro-caging transport primitive in the usual manner. The simply requires a 600 μm move along the Y-axis (Fig9(a)(a)1-4). The second L-part is manipulated next. This time we use the XY stage to move the part to its goal position (Δ X = 600 μm, Δ Y = 200 μm) while it is caged by the micromanipulators (Fig9(a)(b)1-4). Fig9(a)(c)1-4 show the planar manipulation of the T-part, again using the micro-caging grasps and XY stage translations to get the part close to its goal configuration. Then an one-sided-pushing (OSP) primitive [40] is used to accomplish the planar peg-in-the-hole subproblem to place the T-part in its goal location. The square part is then manipulated in 3D with the coordinated micromanipulators. They apply a micro-force-closure grasp and lift the part 100 μm in the Z direction and then the XY stage is translated to allow the placement of the square part over the gap created by the two L-shaped pieces and the T-shaped part (Fig.9(a)(d)1-4). Finally, another 3D transport primitive is used to pick up and place the cross-shaped part on top of the square part (Fig.9(a)(e)1-4). Here, the part is initially picked up 200 μm while it is lowered 100 μm and then released at its goal location. Fig.9(b) shows closeup views of the final assembly with different focal planes in order to see the different layers of the assembly clearer. Some stiction was experienced when releasing the parts after the 3D transport primitives were executed. However, the manipulation plan was successfully accomplished a total of three times.

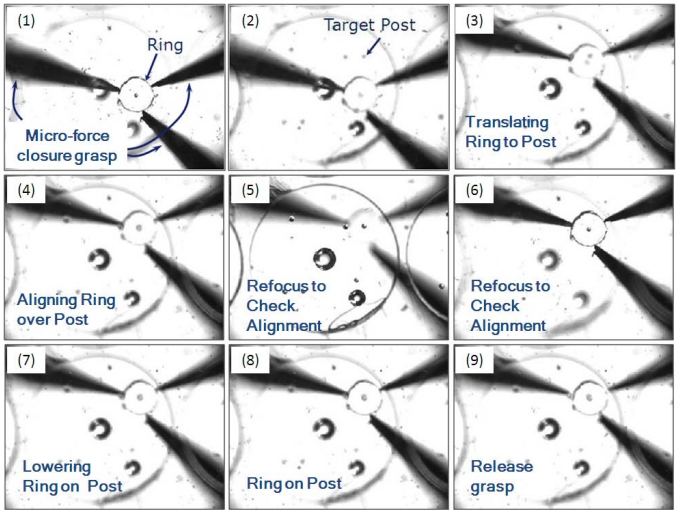

(a) Screenshots of 3D peg-in-the-hole assembly

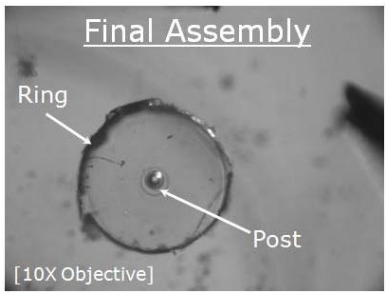

(b) Close-up view of final assembly

FIGURE 8. 3D peg-in-the-hole assembly tests.

DISCUSSION

We postulate that more stable micro-force-closure grasps can be obtained through the use of a select number of dual-tipped-probe endeffectors mounted to the cooperative micromanipulators, based on the work in [42, 43]. Due to the diameter of the shank of our probes, when mounting two probes side-by-side

Copyright © 2012 by ASME

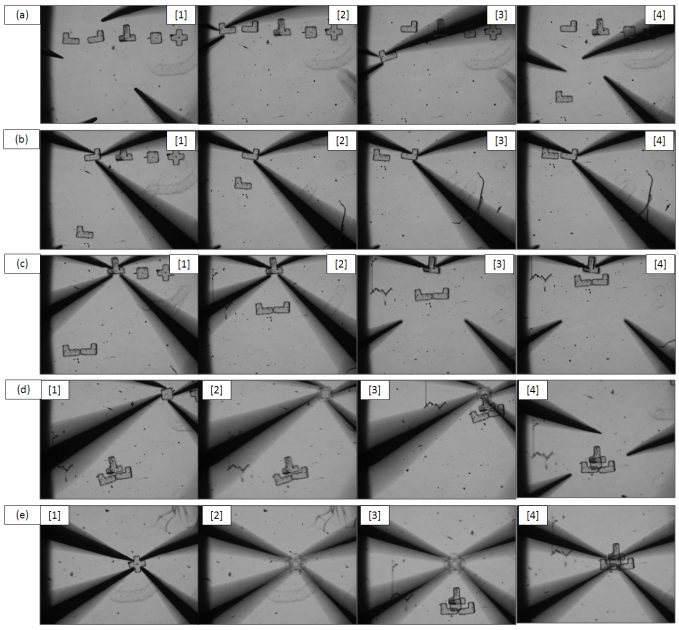

(a) 3D positioning & stacking assembly screenshots

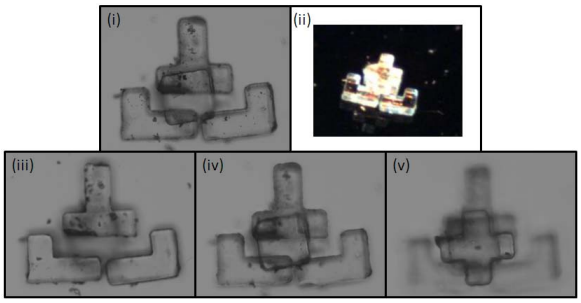

(b) Close-up view of final assembly

FIGURE 9. 3D positioning & stacking assembly tests.

in our system the closest distance that the two probe tips can be apart is about 500 μm. Therefore, we were not able to test this theory with the micro-parts of interest in this study. We will investigate the use of custom dual tip probes in our future work to see if this will help the stability of our grasps.

Also related to stable grasps is micro-force sensing information. Without this force information at the contacts, it is not possible to determine if a proper force distribution is maintained at each contact throughout the transport distance. We will explore both indirect and direct methods of measuring micro-forces in our future work to help close the loop and increase our system performance. This, along with real-time vision feedback, will help us fully automate the assembly process.

Finally, we must comment on control of the part orientation in 3D. Rather than attempt to alter the micro-part's orientation while it is suspended above the substrate, we opt to control the part's orientation in the XY plane with our rotation primitive. This can be applied initially in which a subsequent 3D transport primitive can be administered to the part while it is already in its goal orientation. Similarly, the orientation can also be modified and/or adjusted upon placement of the part back on the substrate (or any planar surface) after a transport task has been finished to obtain the final goal orientation.

CONCLUSION

In conclusion, we have demonstrated a 3D transportion primitive of micro-parts using coordinated micromanipulators and and encoded XY stage. This technique is suitable for 3D micromanipulation and assembly tasks. Experimental results on two canonical examples show the efficacy of our approach with task tolerances of 25 μm and 75 μm, respectively. Future work will look towards fully automating our assembly process through the use of vision feedback, micro-force sensing, and customized probes for increased reliability and overall performance.

ACKNOWLEDGMENT

Part of this work was supported by US Navy / Office of Naval Research Contract # N00014-11-M-0275. The authors would like to thank Wuming Jing for his help with manufacturing the micro-components and test fixtures. We also acknowledge the Micro-Devices Laboratory at Stevens Institute of Technology, Prof. E.H. Yang and Dr. Seongjin Jang for providing the fabrication facility and required equipment training needed for this project.

REFERENCES

[1] Cecil, J., Vasquez, D., and Powell, D., 2005. "A review of gripping and manipulation techniques for micro-assembly applications". International Journal of Production Research, **43**(4), February, pp. 819–828.

[2] Feddema, J., Xavier, P., and Brown, R., 1999. "Micro-assembly planning with van der Waals force". Proceedings of the IEEE International Symposium on Assembly and Task Planning (ISATP '99), July, pp. 32 –38.

[3] Zhou, Y., and Nelson, B., 2000. "The effect of material properties and gripping force on micrograsping". In Proceedings of the IEEE International Conference on Robotics & Automation (ICRA).

[4] Keller, C., 1998. "Microgrippers with integrated actuator and force sensors". In Proceedings of the World Automation Congress, pp. 217–222.

[5] Cecil, J., and Gobinath, N., 2005. "Development of a virtual and physical cell to assemble micro devices". Special Issue of the Journal of Robotics and CIM, August-October, pp. 431–441.

Copyright © 2012 by ASME

[6] Alex, J., Vikramaditya, B., and Nelson, B., 1998. "A virtual reality teleoperator interface for assembly of hybrid MEMS prototypes". Proceedings of DETC98 1998 ASME Engineering Technical Conference, Atlanta, GA, Sept. 13-16.

[7] Kasaya, T., Miyazaki, H., Saito, S., and Sato, T., 1999. "Micro object handling under SEM by vision-based automatic control". Proceedings of the IEEE International conference on Robotics and Automation, Detroit, MI, pp. 2189–2196.

[8] Das, A., Zhang, P., Lee, W., Popa, D., and Stephanou, H., 2007. "μ^3: Multiscale, deterministic micro-nano assembly system for construction of on-wafer microrobots". In IEEE International Conference on Robotics and Automation (ICRA).

[9] Moll, M., Goldberg, K., Erdmann, M., and Fearing, R., 2002. "Orienting micro-scale parts with squeeze and roll primitives". IEEE Int. Conf. on Robotics and Automation, Washington, DC, May 11-15.

[10] Fearing, R., 1995. "Survey of sticking effects for micro parts handling". IEEE/RSJ Int. Conf. on Intelligent Robotics and Sys.(IROS), Pittsburgh, PA, **2**, August 5-9, pp. 212–217.

[11] Boehringer, K., R.Fearing, and Goldberg, K., 1999. Handbook of Industrial Robotics, 2nd Ed. John Wiley and Sons, ch. Microassembly, pp. 1045–1066.

[12] Yang, G., Gaines, J., and Nelson, B., 2001. "A flexible experimental workcell for efficient and reliable wafer-level 3d micro-assembly". In Robotics and Automation, 2001. Proceedings 2001 ICRA. IEEE International Conference on, Vol. 1, pp. 133 – 138 vol.1.

[13] Dechev, N., Cleghorn, W., and Mills, J., 2003. "Microassembly of 3d mems structures utilizing a mems microgripper with a robotic manipulator". In Robotics and Automation, 2003. Proceedings. ICRA '03. IEEE International Conference on, Vol. 3, pp. 3193 – 3199 vol.3.

[14] Dechev, N., Cleghorn, W., and Mills, J., 2004. "Microassembly of 3-d microstructures using a compliant, passive microgripper". Microelectromechanical Systems, Journal of, **13**(2), april, pp. 176 – 189.

[15] Dechev, N., Ren, L., Liu, W., Cleghorn, L., and Mills, J., 2006. "Development of a 6 degree of freedom robotic micromanipulator for use in 3d mems microassembly". In Robotics and Automation, 2006. ICRA 2006. Proceedings 2006 IEEE International Conference on, pp. 281 –288.

[16] Wang, L., Ren, L., Mills, J., and Cleghorn, W., 2007. "Automatic 3d joining in microassembly". In Information Acquisition, 2007. ICIA '07. International Conference on, pp. 292 –297.

[17] Popa, D., Lee, W. H., Murthy, R., Das, A., and Stephanou, H., 2007. "High yield automated mems assembly". In Automation Science and Engineering, 2007. CASE 2007. IEEE International Conference on, pp. 1099 –1104.

[18] Ren, L., Wang, L., Mills, J., and Sun, D., 2007. "3-d automatic microassembly by vision-based control". In Intelligent Robots and Systems, 2007. IROS 2007. IEEE/RSJ International Conference on, pp. 297 –302.

[19] Rabenorosoa, K., Clevy, C., Lutz, P., Bargiel, S., and Gorecki, C., 2009. "A micro-assembly station used for 3d reconfigurable hybrid moems assembly". In Assembly and Manufacturing, 2009. ISAM 2009. IEEE International Symposium on, pp. 95 –100.

[20] Tamadazte, B., Le Fort-Piat, N., Dembele, S., and Marchand, E., 2009. "Microassembly of complex and solid 3d mems by 3d vision-based control". In Intelligent Robots and Systems, 2009. IROS 2009. IEEE/RSJ International Conference on, pp. 3284 –3289.

[21] Tamadazte, B., Arnould, T., Dembele, S., Le Fort-Piat, N., and Marchand, E., 2009. "Real-time vision-based microassembly of 3d mems". In Advanced Intelligent Mechatronics, 2009. AIM 2009. IEEE/ASME International Conference on, pp. 88 –93.

[22] Hui, E., Howe, R., and Rodgers, M., 2000. "Single-step assembly of complex 3-d microstructures". In Micro Electro Mechanical Systems, 2000. MEMS 2000. The Thirteenth Annual International Conference on, pp. 602 –607.

[23] Paik, J. K., Kramer, R. K., and Wood, R. J., 2011. "Stretchable circuits and sensors for robotic origami". In Intelligent Robots and Systems (IROS), 2011 IEEE/RSJ International Conference on, pp. 414 –420.

[24] Sariola, V., Zhou, Q., and Koivo, H. N., 2009. "Three dimensional hybrid microassembly combining robotic microhandling and self-assembly". In Robotics and Automation, 2009. ICRA '09. IEEE International Conference on, pp. 2605 –2610.

[25] Krishnan, S., and Saggere, L., 2007. "A multi-fingered micromechanism for coordinated micro/nano manipulation". J. Micromech. Microeng., **17**, pp. 576–585.

[26] Huang, X., Lv, X., and Wang, M., 2006. "Development of a robotic microassembly system with multi-manipulator cooperation". In Mechatronics and Automation, Proceedings of the 2006 IEEE International Conference on, pp. 1197 – 1201.

[27] Murthy, R., Das, A., and Popa, D., 2006. "Multiscale robotics framework for mems assembly". In Control, Automation, Robotics and Vision, 2006. ICARCV '06. 9th International Conference on, pp. 1 –6.

[28] Das, A., Murthy, R., Popa, D., and Stephanou, H., 2012. "A multiscale assembly and packaging system for manufacturing of complex micro-nano devices". Automation Science and Engineering, IEEE Transactions on, **9**(1), jan., pp. 160 –170.

[29] Wason, J., Wen, J., Choi, Y.-M., Gorman, J., and Dagalakis, N., 2010. "Vision guided multi-probe assembly of 3d microstructures". In Intelligent Robots and Systems (IROS),

Copyright © 2012 by ASME

2010 IEEE/RSJ International Conference on, pp. 5603 – 5609.

[30] Wason, J., Wen, J., and Dagalakis, N., 2011. "Dextrous manipulation of a micropart with multiple compliant probes through visual force feedback". In Robotics and Automation (ICRA), 2011 IEEE International Conference on, pp. 5991 –5996.

[31] Bolopion, A., Xie, H., Haliyo, D., and Regnier, S., 2012. "Haptic teleoperation for 3-d microassembly of spherical objects". Mechatronics, IEEE/ASME Transactions on, **17**(1), feb., pp. 116 –127.

[32] Kosuge, K., Hirata, Y., Kaetsu, H., and Kawabata, K., 1999. "Motion control of multiple autonomous mobile robots handling a large object in coordination". IEEE Int. Conf. on Robotics and Automation, May, pp. 2666–2673.

[33] Rus, D., 1997. "Coordinated manipulation of objects in a plane". Algorithmica, **19**(1), pp. 129–147.

[34] Sugar, T., and Kumar, V., 1999. "Multiple cooperating mobile manipulators". IEEE Int. Conf. on Robotics and Automation, pp. 1538–1543.

[35] Mataric, M., Nilsson, M., and Simsarian, K., 1995. "Cooperative multi-robot box-pushing". IEEE/RSJ Int. Conf. on Intelligent Robots and Systems, pp. 556–561.

[36] Lynch, K., and Mason, M., 1996. "Stable pushing: Mechanics, controllability, and planning". International Journal of Robotics Research, **15**(6), December, pp. 553–556.

[37] Pereira, G., Kumar, V., and Campos, M., 2004. "Decentralized algorithms for multi-robot manipulation via caging". The Int. Journal of Robotics Research, **23**(7/8), pp. 783–795.

[38] Fink, J., Hsieh, M. A., and Kumar, V., 2008. "Multi-robot manipulation via caging in environments with obstacles". In 2008 IEEE International Conference on Robotics and Automation.

[39] Fink, J., Michael, N., and Kumar, V., 2007. "Composition of vector fields for multi-robot manipulation via caging". Robotics: Science and Systems III.

[40] Cappelleri, D., Fatovic, M., and Shah, U., 2011. "Caging micromanipulation for automated microassembly". Proceedings of the IEEE International Conference on Robotics and Automation, Shanghai, China, May.

[41] Cappelleri, D., Fink, J., Mukundakrishnan, B., Kumar, V., and Trinkle, J., 2006. "Designing open-loop plans for planar micro-manipulation". IEEE Int. Conf. on Robotics and Automation, Orlando, FL, May.

[42] Cheng, P., Cappelleri, D., Gavrea, B., and Kumar, V., 2007. "Planning and control of meso-scale manipulation tasks with uncertainties". In Proceedings of Robotics: Science and Systems.

[43] Cappelleri, D., Peng, C., Fink, J., Gavrea, B., and Kumar, V., 2011. "Automated assembly for meso-scale parts". IEEE Transactions on Automation Science and Engineering, **8**(3), July, pp. 598–613.

[44] Peng Cheng, Jonathan Fink, V. K., 2008. "Abstractions and algorithms for cooperative multiple robot planar manipulation". In Proceedings of Robotics: Science and Systems IV.

[45] Cappelleri, D. J., Fatovic, M., and Fu, Z., 2011. "Caging grasps for micromanipulation amp; microassembly". In Intelligent Robots and Systems (IROS), 2011 IEEE/RSJ International Conference on, pp. 925 –930.

[46] Spong, M., Hutchinson, S., and Vidyasagar, M., 2006. Robot Modeling and Control. John Wiley & Sons, Inc.

Copyright © 2012 by ASME